

Photo Rating of Facial Pictures based on Image Segmentation

Arnaud Lienhard, Marion Reinhard, Alice Caplier and Patricia Ladret
GIPSA-lab, Grenoble University, 11, rue des Mathematiques, Grenoble, France

Keywords: Aesthetic Image Quality, Portrait, Categorization, Image Segmentation.

Abstract: A single glance at a face is enough to infer a first impression about someone. With the increasing amount of pictures available, selecting the most suitable picture for a given use is a difficult task. This work focuses on the estimation of the image quality of facial portraits. Some image quality features are extracted such as blur, color representation, illumination and it is shown that concerning facial picture rating, it is better to estimate each feature on the different picture parts (background and foreground). The performance of the proposed image quality estimator is evaluated and compared with a subjective facial picture quality estimation experiment.

1 INTRODUCTION

The development of digital cameras enable people to have access to a constantly growing number of photos. Besides, selecting good-looking images is important in a world where everybody is constantly looking at others pictures. Social psychology studies show that a 100 milliseconds exposure time to a facial portrait is sufficient for people to appraise the subject attractiveness, trustworthiness, competence or aggressiveness (Willis and Todorov, 2006).

The choice of a good facial picture may be application dependent. Profile pictures on social networks are different from pictures selected in a professional purpose. Thus, the features used for automatic aesthetic scoring have to be adapted to the considered application. Aesthetic rules depend on image composition, and evaluating a landscape is different from judging a portrait, where the viewer focuses on the subject's face. That is why finding faces and their contours is important for good estimation performance in portraiture aesthetics.

This work demonstrates the relevance of portraits segmentation in the case of aesthetic scoring, by comparing the performance of a set of features computed either on the entire image or separately on the segmented image. Performance is measured and compared with the results of a subjective quality estimation experiment.

1.1 Related Work

Most of articles dealing with automatic photo rating rely on machine learning techniques. Generally, the whole process is the following. A dataset of pictures rated by humans is created, in order to obtain the ground truth. Then, a set of features is extracted from these pictures. Features are related to photographic rules like the rule of thirds, explain global image properties like the average luminance or describe local image properties. Finally, a learning algorithm is performed to create an image aesthetic model using the extracted features. An example of automatic framework for aesthetic rating of photos is presented in (Datta et al., 2006), and is publicly available on <http://acquine.alipr.com/>.

Many feature sets have been proposed and tested. (Ke et al., 2006) focus merely on high-level features in order to separate poor quality from professional pictures. They design features corresponding to semantic information and abstract concepts such as composition, color or lighting. In their approach, (Luo and Tang, 2008) include image composition features by separating the image into two parts: a region with sharp edges and a blurry region. The blurry region is defined as the background, and features are computed in both regions. However they did not focus on portraits. Then, (Li and Gallagher, 2010) perform face detection and include features related to human faces and their positions: sizes, distances, etc. They compute technical and perceptual features like contrast, blurring or colorfulness on both face and non

face regions. (Khan and Vogel, 2012) adapt spatial composition features to portraiture classification and show the impact of the face position in aesthetic evaluation. However facial portraits require a more accurate segmentation than only separating facial regions from the background. For instance, hair or hats have to be considered when evaluating the visual appeal of a portrait.

1.2 Proposed Method

Our work focuses on frontal facial portraits, which became very common with the proliferation of digital cameras and social media websites.

The idea developed in this article is to show how automatic image segmentation can improve the performance of image quality evaluation. Images are automatically segmented in 4 parts: facial skin, hair, shoulders and background. This segmentation defines two distinct areas. The foreground corresponds to the subject's face, which contains facial skin, hair, and generally the top of the shoulders. The background region is defined as the part of the picture which is not the foreground. This differs from previous work, since (Li and Gallagher, 2010) and (Khan and Vogel, 2012) only performed face detection and did not find the precise contours of the facial regions. For estimation, only few features are considered to emphasize the importance of image segmentation. Considered features are described in Section 3.2.

This paper is organized as follows. Section 2 describes the dataset that has been built and scored by humans in order to have the ground truth. The quality image features considered and the segmentation technique are explained in Section 3. Experimental results of aesthetic quality evaluation are given in Section 4.

2 HUMAN RATING OF FACE IMAGES

2.1 Database

A database containing 125 female and 125 male digital pictures is considered. Half of the images was extracted from free image datasets, such as Labeled Faces in the Wild (Huang and Mattar, 2008) and Caltech Face Dataset (see <http://www.vision.caltech.edu/html-files/archive.html>). The other half of facial images was acquired from private collection.

Most of them are consumer photos. They were cropped to the extremes of the targets head and shoulders (top of the head, bottom of the shoulders, sides of

hair or ears) and standardized for size (from 240×148 to 240×320).

The face in the picture is always right-side-up and centered. A large variety of photos is considered: all types of gaze and expression, facial hair styles, presence of accessories (earrings, eyeglasses, hat and visible make-up), clothing, etc.

2.2 Human Picture Rating

Twenty-five men and women, mostly aged from 20 to 30, were asked to judge facial photos using a discrete scale from 1 (very low quality) to 6 (very high quality). They were instructed that they would be seeing a series of faces randomly presented on a computer screen and that their task is to assess the aesthetic quality of each of the images displayed. Instructions were the same for each participant: *A picture will be judged as very aesthetic when the numerous aspects that qualify it (framing, luminosity, contrast, blooming, balance between the components, etc.) are of good quality. Please indicate the aesthetic quality of the picture, using a scale from 1 (very bad quality) to 6 (excellent quality).*

Even if only facial portraits are considered, facial beauty is not part of the criteria and the final objective is to evaluate the global aesthetic quality of the picture only.

2.3 Preliminary Results

Each image is associated with a mean score over the 25 votes and a distribution of scores corresponding to individual votes. These scores rank from 1.36 to 5.36 (Mean of 3.21, Standard Deviation of 0.73). The distribution is largely Gaussian and all the possible votes are represented, as presented in Figure 1. To estimate the reliability of the test scores, Cronbach's Alpha (Cronbach, 1951) is computed: $\alpha = 0.99$. α ranges between 0 and 1 and it is commonly accepted that $\alpha > 0.9$ means a very high internal consistency of the chosen scale.

These scores are considered as the ground truth and are used to evaluate the performance of the image quality estimator proposed in Section 4.

3 IMAGE SEGMENTATION AND IMAGE QUALITY FEATURES

Finding the facial skin area may help a lot for aesthetic scoring in portraits. Computing blur or brightness values in this special location may greatly differ

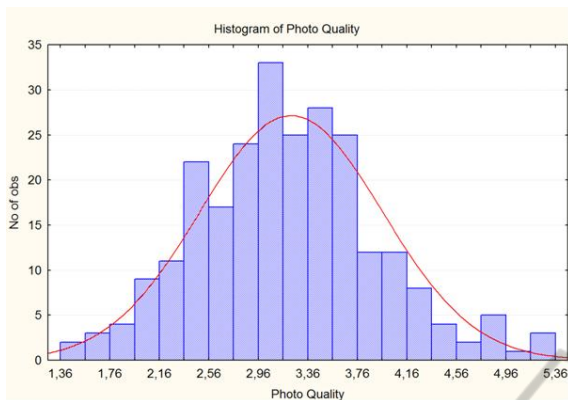


Figure 1: Histogram of image aesthetic quality mean rating.

from the global blur or brightness values, changing our perception of the global image aesthetic.

3.1 Image Segmentation

3.1.1 Face and Facial Features Detection

Face bounding box detection is performed by using the Viola-Jones algorithm described in (Viola and Jones, 2001). It has been implemented in C++ using the OpenCV library, version 2.4.3. When several faces are detected, only the biggest one is kept. Detection performance is good since all the faces among the dataset of 250 images are detected.

The same algorithm is applied on the face bounding box to detect eyes (left and right eyes are detected separately), nose and mouth. Facial features detection process has been tested on the LFW dataset (about 13,000 images) and obtained 89% of correct feature extraction.

3.1.2 Facial Image Segmentation

The Viola-Jones algorithm provides bounding boxes for face and facial features. Since our goal is to show that a fine segmentation of the face is required for a good image quality estimation, the proposed method for face segmentation is presented below. It is based on the results obtained after applying the Viola-Jones algorithm.

In order to detect the location of facial contours, the advantages of two techniques are combined (see Figure 3). First, a histogram containing the values of skin pixels in the area defined by the facial features is created. After normalization, for each pixel value in the entire image, the probability to be part of facial skin is computed. Many skin detection models have been developed, for example (Jones and Rehg, 1999)

used *BGR* color space and constructed histogram using hand labeled skin regions. Hue and saturation channels from the *HSV* color space are often used. However hue becomes less discriminant when dealing with underexposed images or with different skin colors. For that reason, red and saturation channels from respectively *BGR* and *HSV* color spaces are used.

A segmentation algorithm is performed on the probability image obtained from the histogram model, to separate skin and non skin areas. Watershed is widely used to solve segmentation problems. The version implemented in OpenCV and inspired by (Beucher and Meyer, 1993) is chosen. Skin area is used as a seed for facial skin region, and image corners are used as seeds for the non skin area. Performing Watershed on the histogram back projection (see Figure 3) prevents the algorithm from setting non skin pixels to the facial skin area, and increases the initial skin area defined by facial feature detection.

Using this new skin area enables us to compute a more precise histogram, which provides a better seed for the next iteration of segmentation. Iterating this several times often creates fine contours. The whole process is iterated 20 times.

To segment hair, we use exactly the same technique than for skin segmentation. The only difference is the initialization step. Since we already have found the skin area, and knowing that hair is above facial skin, the area that is used to create the hair model is defined. Same operation is done for shoulder segmentation: the initial shoulder location is the image part below facial skin region.

Finally, the background region is defined as the remaining region, while the foreground region is the addition of facial skin, hair and shoulders areas. Some segmentation results are provided in Figure 2.



Figure 2: First row presents nice segmentation results, while second row shows segmentation on more challenging images: presence of sunglasses, unclear limitations between skin, hair and background, etc.

3.2 Image Quality Features

6 measurements related to image quality are implemented and are computed separately either in the whole image or in subregions.

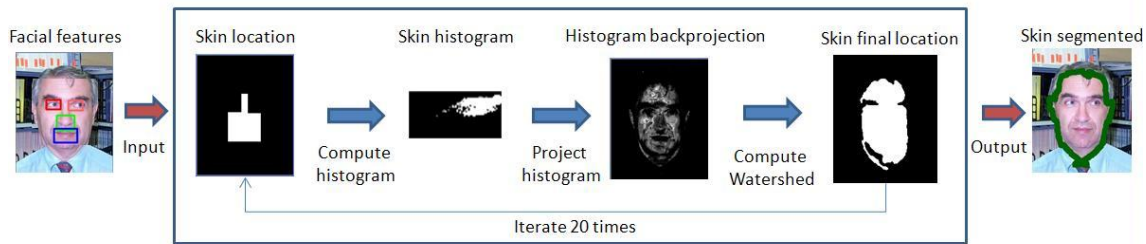


Figure 3: Presentation of the segmentation process.

3.2.1 Blur

Blurry images are generally correlated to poor quality. However this is not completely true with portraits: if the face contains sharp edges, the background may be blurred without affecting the global image aesthetic quality. It may even enhance the visual appeal of the picture, by increasing the contrast between face and background.

The blur value is computed using the procedure described in (Crete and Dolmiere, 2007). It is close to 0 for a sharp image, and close to 1 for a blurred image. The idea is to blur the initial image and to compare the intensity variation of neighboring pixels in both initial and blurred images. Figure 4 briefly describes the blur estimation principle. A couple of images and their blur values are presented in Figure 5.

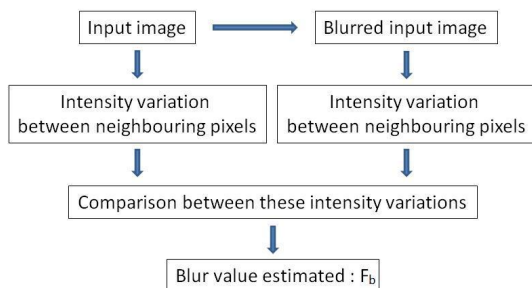


Figure 4: Simplified flowchart of the blur estimation principle described in (Crete and Dolmiere, 2007).



Figure 5: Examples of high and low blur levels, computed in the entire image. Blur from left to right: $F_b = 0.29$ and $F_b = 0.62$. Ground truth quality scores are 4.4 and 2.0, respectively.

3.2.2 Color Count

The number of colors in an image may have an impact on the global aesthetic feeling. Figure 6 shows example of images with high and low colorfulness values. Many articles use hue counts (Ke et al., 2006) or the number of colors represented in the RGB color space (Luo and Tang, 2008). We chose to use the *Lab* color space, since it is designed to approximate human vision, and the color channels (*a* and *b*) are separated from the luminance channel (*L*).

A 2-dimensional histogram H is computed from both color channels, using 16×16 bins. We do not take into account pixels with too low or too high luminance values L ($L < 40$ or $L > 240$), since their color values are not significant. The histogram is normalized in order to have a maximum value of 1. Let $H(i, j)$ be the frequency of pixels such that the *a* and *b* color values belong to bins *i* and *j*, respectively. We define $|C|$ as the number of pairs (i, j) such that $H(i, j) > \alpha$. α is set to 0.001. The color count is finally:

$$F_c = |C|/256 \times 100\% \quad (1)$$

F_c equals to 1 when all the possible colors are represented, and is close to 0 otherwise.



Figure 6: Pictures with many different colors have a higher colorfulness value than pictures with a uniform background. From left to right: $F_c = 0.11$ and $F_c = 0.02$. Ground truth quality scores are 3.4 and 2.0, respectively.

3.2.3 Illumination and Saturation

Professional photographers often adapt the brightness of a picture, and make the face illumination differ-

ent from the background enlightening. The overall brightness should neither be too high nor too low. In this work, brightness average and standard deviation are considered. Computing these feature values can be done by considering the value channel V from the HSV color space.

The same operation is done for the saturation channel S . Saturation is a color purity indicator. Saturation average and standard deviation are computed from the saturation channel of the HSV color space.

After computation, the following values are obtained:

- μ_V , brightness mean
- σ_V , brightness standard deviation
- μ_S , saturation mean
- σ_S , saturation standard deviation

3.2.4 Final Feature Set

The final set of measurements \mathcal{F} is

$$\mathcal{F} = (F_b, F_c, \mu_V, \sigma_V, \mu_S, \sigma_S)$$

This measurements are computed in the 6 following regions:

1. Entire image
2. Foreground: addition of skin, hair and shoulders
3. Background
4. Facial skin area
5. Hair area
6. Shoulders area

This makes a total of 6×6 features. In the experiments, the feature set \mathcal{F}_i is the set \mathcal{F} computed on the region i . For example, \mathcal{F}_1 represents the set of features \mathcal{F} evaluated on the entire image.

4 AUTOMATIC AESTHETIC QUALITY ESTIMATION

In this section, classification and image scoring are performed to show how much segmentation improves the quality evaluation. Feature are tested separately in section 4.2. In all the experiments, results are compared with ground truth scores. 3 feature set combinations are used to show segmentation influence:

1. Feature set \mathcal{F}_1 is used to have an idea of the global features performance, when they are computed on the entire image.

2. Feature sets \mathcal{F}_2 (foreground) and \mathcal{F}_3 (background) are used to demonstrate the segmentation influence.

3. Finally, feature sets \mathcal{F}_3 (background), \mathcal{F}_4 (face), \mathcal{F}_5 (hair) and \mathcal{F}_6 (shoulders) are used to show the performance improvements when the foreground is separated in 3 parts.

We used the k-fold cross validation technique, with $k = 10$. Images were removed when we could not extract all of the facial features (e.g. images with large sunglasses).

4.1 Influence of Segmentation on Classification

The main objective of picture classification is to separate good looking images from bad pictures. Support vector machines (SVM) are widely used to perform categorization applied to image aesthetic evaluation (Datta et al., 2007). To classify the pictures in several groups, SVM with a Gaussian Kernel is performed. Performance is evaluated by the Cross-Category Error (CCE)

$$CCE_i = \frac{1}{N_t} \sum_{n=1}^{N_t} I(\hat{c}_n - c_n = i)$$

and the Multi-Category Error (MCE)

$$MCE = \sum_{i=-(N_c-1)}^{N_c-1} |i| CCE(i)$$

where N_t is the number of test images, N_c the number of classes, \hat{c}_n the ground truth classification described in Section 2.3, c_n the predicted classification. i is the difference between ground truth and predicted classification and $I(\cdot)$ is the indicator function.

Since random training and testing sets are used, and due to the limited amount of images available in the dataset, all of the experiments are repeated 10 times with various sets. Then, the average performance is displayed.

4.1.1 2-Class Classification

2-class categorization is used to separate high and low quality images. Images below the median aesthetic ground truth score are labeled as group 0, and images above as group 1. The median aesthetic score is around 3.2 (see Figure 1). Results of the 3 experiments described in Section 4 are presented in Table 1.

It has to be noticed that results are significantly above the performance of a random classifier. Results show that segmenting the image can help a lot to classify

Table 1: Experimental results for 2-class categorization. CCE_{-1} is the number of overrated images, CCE_0 is the number of good classification and CCE_1 is the number of underrated images. Performance is the good classification rate.

F. sets	Perf.	CCE_{-1}	CCE_0	CCE_1
\mathcal{F}_1	75.2%	22	128	20
$\mathcal{F}_2, \mathcal{F}_3$	77.7%	23	132	15
$\mathcal{F}_3 \dots \mathcal{F}_6$	83.7%	20	141	9

images in two categories. After segmentation the good classification rate increases from 75% to almost 84%.

4.1.2 3-Class Classification

3-Class categorization is an interesting problem, since we often want to separate highly rated or remove poorly rated images. For this task, 3 groups of about 50 images are used. The first group contains the 50 lowest aesthetic score, the second group contains images with medium aesthetic score (between 3 and 3.4). The last group contains only high-rated images. We are using a total of 160 images. Images have label 0 for low aesthetic quality, 1 for medium quality and 2 for high quality.

The same experiments are conducted, and classification performance is presented in Table 2.

Table 2: Experimental results for 3-class categorization. MCE measures the number of misclassifications.

F. sets	Performance	MCE
\mathcal{F}_1	54.3%	85
$\mathcal{F}_2, \mathcal{F}_3$	58%	80
$\mathcal{F}_3 \dots \mathcal{F}_6$	60.0%	78

A random classifier would have a correct classification rate of about 33%. Again, segmentation helps for 3-Class categorization, since performance increases from 54% to 60% after segmentation.

4.2 Influence of Image Quality Features

To have an idea of features influence, 2-Class categorization is performed using only one feature at a time. Classification performance is reported in Table 3 for the 6 features evaluated on the entire image (\mathcal{F}_1), the foreground region (\mathcal{F}_2) and the background region (\mathcal{F}_3).

The ground truth quality score is highly correlated with the blur value F_b : there is about 70% of correct classification for the dataset considered. This score change with respect to the image region considered. The blur value is more discriminant when computed on the foreground region (71%, and only 66% for the

Table 3: Features good classification rates (%).

F. set	F_b	F_c	μ_V	σ_V	μ_S	σ_S
\mathcal{F}_1	70	52	55	59	54	51
\mathcal{F}_2	71	50	57	52	57	51
\mathcal{F}_3	66	44	49	55	50	51

background region), which is the most important part of a portrait and should not be blurry. It is almost the performance obtained by using the entire set \mathcal{F}_1 (75%).

Other features like the color count F_c or the saturation standard deviation σ_S have lower good classification rates, with respectively 52 and 51% when computed on the entire image, which is not significantly higher than the 50% obtained using a random classifier.

In a portrait, a nice illumination for the subject is important and face illumination has an impact on image quality: the brightness mean μ_V computed on the foreground region has a good classification rate of 57%. The same feature evaluated on the background region has a lower score of 49%.

4.3 Influence of Segmentation on Image Quality Scoring

In this section, the results of quality scoring with and without image segmentation are presented. To this end, a Support Vector Regression (SVR) is performed. All of the images available in the dataset are used: 90% for learning and 10% for testing. An SVR implementation is given in the OpenCV library.

Measuring the regression performance is slightly more difficult. A model which always predicts the average value will have a nice mean error if many images have aesthetic scores close to this mean. After regression, the predicted data should be as close as possible to the expected values.

To measure prediction performance, 3 criteria are used. The Mean Squared Error E quantifies the difference between ground truth and predicted scores. Let \hat{s}_n be the ground truth and s_n the predicted score of picture n :

$$E = \frac{1}{N_t} \sum_{n=1}^{N_t} (\hat{s}_n - s_n)^2$$

The Pearson correlation R is defined as

$$R = \frac{\sum_{n=1}^{N_t} (\hat{s}_n - \bar{\hat{s}}) \cdot (s_n - \bar{s})}{\sqrt{\sum_{n=1}^{N_t} (\hat{s}_n - \bar{\hat{s}})^2} \cdot \sqrt{\sum_{n=1}^{N_t} (s_n - \bar{s})^2}}$$

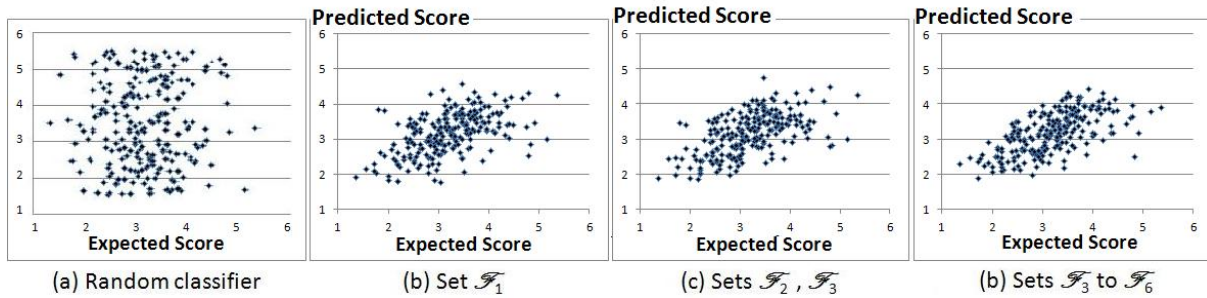


Figure 7: Prediction results for segmented and non segmented images.

where $\hat{s} = \frac{1}{N_t} \sum_{n=1}^{N_t} \hat{s}_n$ and $\bar{s} = \frac{1}{N_t} \sum_{n=1}^{N_t} s_n$. Finally the Spearman rank correlation ρ is computed

$$\rho = 1 - \frac{6 \sum_{n=1}^{N_t} d_n^2}{N_t(N_t^2 - 1)}$$

where $d_n = \hat{s}_n - s_n$ is the rank difference between variables. While Pearson’s measure quantifies how much the data are linearly correlated, Spearman’s rank correlation tells if the data are monotonically correlated. Values close to 1 result from correlated data and 0 means that the data are not correlated.

Figure 7 shows the prediction results after experiments and Table 4 displays the 3 coefficients computed from the 3 experiments. An additional graph is presented to show the result of a random computation. A perfect prediction would have only points on the line $y = x$.

Table 4: Experimental results of regression.

Experiment	Error E	Corr. R	Corr. ρ
\mathcal{F}_1	0.59	0.52	0.53
$\mathcal{F}_2, \mathcal{F}_3$	0.58	0.55	0.56
$\mathcal{F}_3 \dots \mathcal{F}_6$	0.55	0.61	0.64

Without any segmentation (Figure 7 b), the regression results are a lot better than randomized prediction. However high and low scores may be far from ground truth. Since the more common usages of aesthetic scoring are either eliminating low quality images or selecting high quality images, this is not a satisfying result. Segmentations (Figures 7 c and d) don’t reduce a lot the mean squared error (from 0.59 to 0.55, but reduce errors for extremes scores.

Image segmentation increases the correlation coefficients values from about 0.5 to 0.6: the prediction is more accurate. Examples of very high and very low quality images are presented in Figure 8 with their ground truth and predicted scores.



Figure 8: a) Highest ground truth scores. b) Lowest ground truth scores. c) Highest predicted scores. d) Lowest predicted scores.

4.4 Validation on a Larger Dataset

In order to check the robustness of the method, we have been looking for a larger dataset, containing frontal facial images. Many photo sharing portals exist, like *Photo.net* or *DPChallenge.com*. These websites allow people to share pictures and to score others pictures. Datasets have been created by extracting such images with their scores. We chose to extract a subset of the AVA database presented in (Murray, 2012), containing 250,000 images extracted from *DPChallenge*. About 800 coloured frontal facial images were found, as described in Section 2.1.

To compare with the previous experiments, 2-class categorization is performed using the 250 images with the lowest and highest aesthetic scores. Results are presented in Table 5.

Again, good classification rate increases after segmentation, from 55 to 63%. We still have interesting results with simple features. However results are worse than for the previous dataset. This may be explained by the use of more sophisticated photography

Table 5: Experimental results for 2-class categorization of the second dataset (500 images).

F. sets	Perf.	CCE_{-1}	CCE_0	CCE_1
\mathcal{F}_1	55.3%	110	275	115
$\mathcal{F}_2, \mathcal{F}_3$	58.6%	99	294	107
$\mathcal{F}_3 \dots \mathcal{F}_6$	63.0%	98	315	87

techniques in this dataset, making the features less effective. Moreover, it contains almost no blurry images and performing 2-class categorization using only the blur value computed on the foreground region leads to an average performance of only 52.3% (71% for the previous dataset). Pictures have a lower score variance (0.75 on a 1 to 10 scale) which makes the categorization difficult.

5 CONCLUSIONS

In this work we proposed a method based on image segmentation to explore aesthetics in portraits. A few features were extracted, and image segmentation techniques improved evaluation performance in both categorization and score ranking tasks.

In the experiments, only a couple of hundred images have been used and it is not sufficient to create accurate models, especially for aesthetic scoring. Gathering more images from different sharing portals and other datasets may help a lot.

The features described and computed are simple descriptors. They can be combined with generic image descriptors, other data related to portraits, etc. Facial features like hair color, background composition and textures, make-up and facial expressions, as well as presence of hats and glasses can be used to provide more accurate scoring.

Implementing new relevant features will be part of future work. Comparison between several learning techniques will be performed and additional regions explored (e.g. eyes and mouth locations).

This will be a first step in evaluating facial portraits with respect to other criteria like attractiveness, competence, aggressiveness.

REFERENCES

Beucher, S. and Meyer, F. (1993). The morphological approach to segmentation: the watershed transformation. *Mathematical Morphology in Image Processing*, pages 433–481.

Crete, F. and Dolmiere, T. (2007). The blur effect: perception and estimation with a new no-reference perceptual blur metric. *Proc. of the SPIE*, 6492.

Cronbach, L. (1951). Coefficient alpha and the internal structure of tests. *Psychometrika*, 16(3).

Datta, R., Joshi, D., Li, J., and Wang, J. Z. (2006). Studying Aesthetics in Photographic Images Using a Computational Approach. *ECCV*, pages 288–301.

Datta, R., Li, J., and Wang, J. Z. (2007). Learning the consensus on visual quality for next-generation image management. *Proc. of the 15th international conference on Multimedia*, pages 533–536.

Huang, G. and Mattar, M. (2008). Labeled faces in the wild: A database for studying face recognition in unconstrained environments. *Workshop on Faces in 'Real-Life' Images: Detection, Alignment, and Recognition*, pages 1–11.

Jones, M. and Rehg, J. (1999). Statistical color models with application to skin detection. *CVPR*, 1:274–280.

Ke, Y., Tang, X., and Jing, F. (2006). The design of high-level features for photo quality assessment. *CVPR*, 1:419–426.

Khan, S. and Vogel, D. (2012). Evaluating visual aesthetics in photographic portraiture. *Proc. of the Eighth Annual Symposium on Computational Aesthetics in Graphics, Visualization, and Imaging (CAE '12)*, pages 1–8.

Li, C. and Gallagher, A. (2010). Aesthetic quality assessment of consumer photos with faces. *ICIP*, pages 3221 – 3224.

Luo, Y. and Tang, X. (2008). Photo and video quality evaluation: Focusing on the subject. *ECCV*, pages 386–399.

Murray, N. (2012). AVA: A large-scale database for aesthetic visual analysis. *CVPR*, 0:2408–2415.

Viola, P. and Jones, M. (2001). Rapid object detection using a boosted cascade of simple features. *CVPR*, 1:511–518.

Willis, J. and Todorov, A. (2006). Making Up Your Mind After a 100-Ms Exposure to a Face. *Psychological Science*, 17(7):592–598.